1996 ASME PVP Conference, July 21-26, Montreal, Canada

CONF-960706--7

# A FINITE ELEMENT MODEL FOR RESIDUAL STRESS IN REPAIR WELDS

**Z. Feng**
Edison Welding Institute, Columbus OH

**X.-L. Wang, S. Spooner, G.M. Goodwin,**
**P.J. Maziasz, C.R. Hubbard and T. Zacharia**
Oak Ridge National Laboratory, Oak Ridge TN

## ABSTRACT

This paper describes a three-dimensional finite element model for calculation of the residual stress distribution caused by repair welding. Special user subroutines were developed to simulate the continuous deposition of filler metal during welding. The model was then tested by simulating the residual stress/strain field of a FeAl weld overlay clad on a $2^1/_4$Cr-1Mo steel plate, for which neutron diffraction measurement data of the residual strain field were available. It is shown that the calculated residual stress distribution was consistent with that determined with neutron diffraction. High tensile residual stresses in both the longitudinal and transverse directions were observed around the weld toe at the end of the weld. The strong spatial dependency of the residual stresses in the region around the weld demonstrates that the common two-dimensional cross-section finite element models should not be used for repair welding analysis.

## INTRODUCTION

There has been significant advancement in the development of computational models to evaluate residual stresses in welded structures (Hibbitt and Marcal, 1973; Argyris, et al., 1982; Lindgren and Karlsson, 1982; and Goldak, 1989). Although three-dimensional models are available (Karlsson and Josefson, 1990; Tekriwal and Mazumder, 1989), most practical calculations have been carried out using various two-dimensional cross-section models, because of the limitation of computational resources in the past. The cross-section models are based on the hypothesis that the deformation of a weld is two dimensional, satisfying the plane strain or generalized plane strain conditions. It assumes that there is no out-of-plane shear stress components, and the cross section plane does not warp during heating and cooling cycle of welding. These assumptions imply that the cross-section models are limited to the situations where geometrical similarity exists along the weld direction, for example, in the regions around the middle sections of long, straight single and multipass welds (Josefson, 1986; Leung and Pick, 1990; and Shim et al. 1992). The calculated residual stress results were found in reasonable agreement with experimental measurements in those cases. Another type of problem that has been investigated with two-dimension models is spot welds (Mahin et al., 1991; and Feng et al., 1995), where axisymmetry exists. Again, in both studies, the calculated residual elastic strain distributions were in reasonable agreement with the experimental data obtained with neutron diffraction.

In simulating welding processes that involve filler metal deposition (for example, GMAW and SMAW), proper treatment of the continuous filler metal deposition requires special considerations in the formulation of numerical solution strategy. A variety of element rebirth/re-activating techniques has been attempted to address this issue. In general, determination of the element reactivation sequence prior to an analysis is needed. It is also common to reactivate all the elements representing one weld pass at once either before that pass is to be deposited or at a predetermined time/temperature instant during welding of the pass, in order to further reduce the complexity associated with the gradual element reactivation scheme that is physically more appropriate. This procedure is quite tedious but generally manageable for the two-dimensional models.

There have been few models that deal with repair welding situations. In many instances, cracks initiate at the regions around the weld ends. It is thus important for an FE model to provide realistic residual stress information at these critical locations. It is expected that there would be significant shear stress components normal to the cross-section in the regions around the weld ends. Thus, the two-dimensional cross-section models do not apply (Goldak et al., 1986 and Wang et al., 1995), and three-dimensional models are necessary. In such cases, elements representing the filler metal need to be individually reactivated only when they enter the moving weld pool, in order to simulate the physics of the process appropriately. The

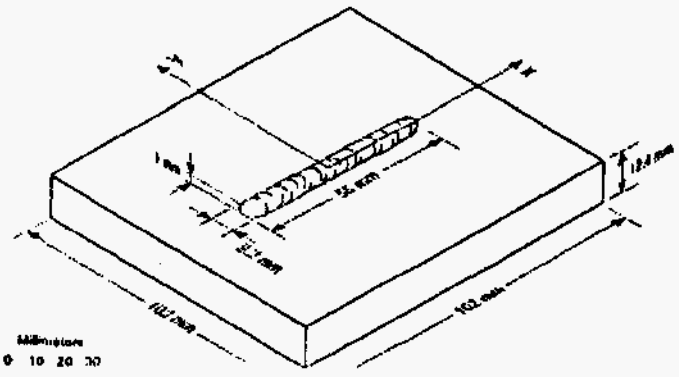

**Figure 1 A schematic drawing of the specimen used for residual stress analysis.**

aforementioned manual element rebirth procedure in principle applies to simulate the continuous deposition of filler metal as the welding arc moves through. In practice, however, it becomes extremely difficult to implement in three-dimensional models (Tekriwal and Mazumder, 1989), because the elements representing one weld pass cannot be re-activated all together at once. In addition, numerical difficulties may also occur in the mechanical analysis upon element reactivation due to the displacement mismatch between the deformed elements representing the weld that already exist and the fresh undeformed elements that are just reactivated. In some other studies, the continuous metal deposition is simply ignored by leaving the filler metal elements in the solution domain all the time (Dighde et al., 1993). A problem with such treatment is that the high stiffness of a filler metal element prior to its deposition disturbs the deformation patterns in the adjacent region.

An objective of this study is thus to develop a finite element modeling algorithm which handles the continuous metal deposition automatically. This is achieved by the use of a special user material property subroutine in which elements representing the weld metal are assigned to have the rigidity of the air. The true material stiffness is restored only when the element enters the moving weld pool. The algorithm is general and not limited to the repair welding situation. It can be easily adopted in other single or multipass welding applications. The algorithm was implemented in a commercial finite element code, ABAQUS, by means of user subroutines. The model was then tested in this study by simulating the residual stress/strain field of a FeAl weld overlay clad on a 2¼Cr-1Mo steel plate, for which neutron diffraction measurement data of the residual strain field were available. It is shown that the calculated residual stress distribution was consistent with that determined with neutron diffraction.

## MATERIALS AND WELDING

A schematic drawing of the specimen used for residual stress analysis is shown in Figure 1. The size of the 2-1/4Cr-1Mo steel plate was 101.6x101.6x12.7 mm (4x4x1/2"). The steel plate was given a standard normalization (1 hr. at 900°C + 1 hr. at 700°C) heat-treatment prior to welding. The weld filler metal was an FeAl alloy with a nominal composition of Fe-34.0Al-4.4Cr (at %) [Fe-20Al-5Cr (wt%)]. FeAl was clad on the surface of the steel using the manual GTAW process with stringer bead. The welding direction in Figure 1 was from left to right. The welding parameters varied during welding because of the nature of manual welding. The travel speed, current and voltage ranged between 0.84-1.7 mm/s (2-4 ipm), 100-120A, and 10-12V, respectively. Averaged values were used in the finite element model. To avoid the formation of cracks in the weld metal, the steel plate was preheated to 350°C. The weld bead, approximately 9.2 mm wide and 55 mm long, was located on the center of the steel plate surface.

## NEUTRON DIFFRACTION

The determination of residual stresses by neutron diffraction is based on the measurement of the lattice strain, ε, using a Bragg reflection from the crystalline specimens (Spooner et al., 1993 and Root et al., 1993). According to Bragg's law,

$$\lambda = 2d\sin\theta \tag{1}$$

where λ is the neutron wavelength, d and 2θ are, respectively, the lattice spacing and diffraction angle of the reflection of interest. From the measured lattice spacing, the lattice strain is calculated using the equation,

$$\varepsilon = \frac{d - d_0}{d_0} \tag{2}$$

where $d_0$ is the unstressed lattice spacing. For a given specimen orientation, the strain component parallel to the scattering vector is measured. Strain mapping is accomplished using a three-dimensional translation stage mounted on the sample table of the neutron diffractometer. Figure 2 illustrates the experimental arrangement in the present study.

The residual stress measurements were conducted at the High Flux Isotope Reactor of Oak Ridge National Laboratory. Incident neutrons of 1.614 Å wavelength were selected from the (1 1 0) reflection of a beryllium single crystal monochromator at a take-off angle of 90°. For both the steel plate and the FeAl weld, diffraction from the (2 1 1) crystallographic plane was used. At each location, a diffraction peak profile was recorded with an ORDELA linear position-sensitive detector. The recorded peak profile was fitted with a Gaussian function to yield the position (2θ), intensity, and the width of the peak. For mapping in the steel, vertical slits of dimensions 2x2 $mm^2$ and 2x30 $mm^2$ were inserted before and after the specimen, respectively, defining a sampling volume of 2x2x2 $mm^3$. A 6x6x50 $mm^3$ coupon cut from an identical steel plate was used to determine the $d_0$ of the steel. For mapping in the FeAl weld, the sampling volume

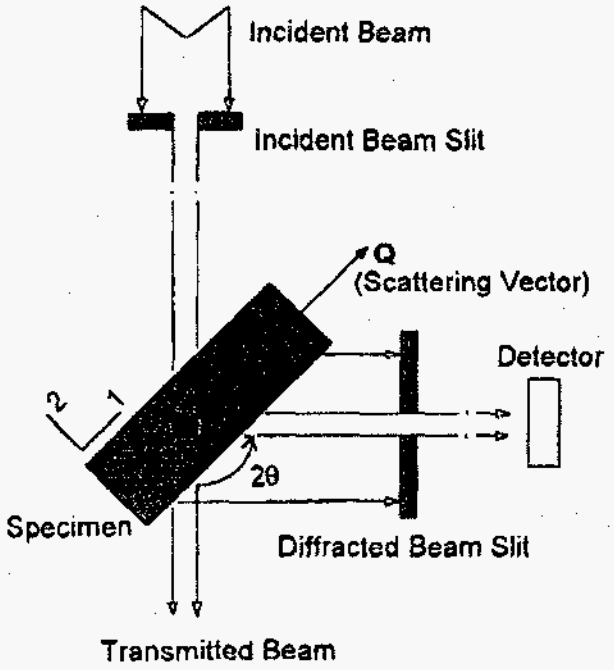


**Figure 2 Experimental setup for neutron diffraction based strain mapping.**

was 2x2x5 $mm^3$, defined by pair of vertical slits with the dimensions 2x5 $mm^2$ and 2x30 $mm^2$, respectively. The composition of the FeAl weld metal changed from that of FeAl filler rod due to the dilution between the base steel and the FeAl filler. A reference specimen for the FeAl weld cannot be made without cutting the specimen. However, since the thickness of the weld-overlay was small (~1 mm), it is reasonable to assume that the residual stress state in the FeAl weld is bi-axial. In this case, residual strains in the FeAl weld were obtained without the need of a reference specimen.

## FE MODEL

The thermomechanical behavior of the weldment during welding can be simulated using the uncoupled formulation, because the dimensional changes are negligible and the mechanical work done is insignificant compared to the thermal energy from the welding arc (Hibbitt and Marcal, 1972). A recent study (Feng et al., 1995) using both the coupled and uncoupled models for the same GTAW spot weld on steel disk provides further evidence that supports the validity of the uncoupled approach.

In the uncoupled formulation, the heat transfer analysis was decoupled from the mechanical analysis. However, the formulation considered the contributions of the transient temperature field to stress analysis through thermal expansion and volumetric change, as well as temperature-dependency of thermophysical and mechanical properties. The solution procedure was in principle similar to those used in 2-D FE analyses of welding residual stress and distortion problems (Josefson, 1986; and Feng et al., 1995). The temperature history during welding and subsequent cooling of the weldment was calculated first, independent from the mechanical analysis. The temperature history as calculated in the heat transfer analysis was then used as a thermal load in the subsequent mechanical calculation.

The finite element model was constructed according to the above experimental essentials. The weldment was meshed using 8 node brick type elements. For the mechanical analysis, reduced integration and hourglass control were adopted. The model consisted of about 4500 elements, with finer elements in the weld and adjacent regions.

Temperature-dependent thermophysical and mechanical properties were used. They were collected from various sources (Maziasz et al., 1992; Porter and Maziasz, 1993; Schneibel, 1994; and ASM, 1990). For simplicity, the effect of weld dilution on the properties changes was ignored. The thermal conductivity of both steel and FeAl above their respective melting temperatures was artificially increased to compensate for the convective heat transfer effect in the molting weld pool. The mechanical constitutive behavior was assumed to be rate-independent elasto-plastic ones obeying the von Mises yield criteria and associated flow rules.

In the heat transfer analysis, the heat from the moving welding arc was applied as a volumetric heat source, taking an ellipsoidal form proposed by Goldak et al. (1984):

$$q = \frac{6\sqrt{3}\eta VI}{\pi\sqrt{\pi}abc}\exp\left[-3\left(\frac{x^2}{a^2}+\frac{y^2}{b^2}+\frac{z^2}{c^2}\right)\right] \qquad (3)$$

where, the arc efficiency, η, was assumed to be 70% for the manual GTAW process. The characteristic parameters (a, b, c) were taken to be 4.5, 4.5, and 2.5 mm respectively. The coordinate system is defined in Figure 1. The Z=0 plane is coincident with the interface between the steel plate and the FeAl weld. The heat flux was only applied to the $Z<0$ semi-infinite space (i.e., in the steel plate only), due to energy conservation consideration (Goldak et al., 1984).

The elements that represent the weld bead always exist during the heat transfer analysis. However, the thermal conductivity and the heat capacity of these elements were first assigned to small values to represent the existence of the air, using the field variable concept in ABAQUS. They were switched back to the actual properties of FeAl on integration point basis when an integration point entered a region of 10 mm in diameter from the center of the moving welding arc, as the welding arc passed through these elements during the course of welding. This treatment implies that the effects of convection and radiation in the region occupied by the weld elements located in front of the weld pool were not included in the model.

Similarly, in the mechanical analysis, the model first assigned a set of artificial, very soft properties for elements that are to be welded later. The elements were then switched back to the actual properties on integration point basis as the material at the integration point began to solidify from the weld pool. In order to avoid numerical convergence problems, the switching was done based on the temperature at integration point, not on the location relative to the center of the welding arc. The reason is that the size of the weld pool varied during welding because of the initial and terminal transient temperature stages at the weld ends. In addition, the unrealistic plastic strains accumulated prior to the switching were eliminated within the

increment in which the switching took place. A UMAT user subroutine was written for this purpose.

## RESULTS

### Comparison of Elastic Strains

Comparisons between the neutron diffraction measurement and the finite element modeling results are made on the elastic strain basis. As noted by Mahin et al. (1991), this is to avoid ambiguities in converting stresses from the measured elastic strains.

Figure 3 shows the comparison of the longitudinal elastic strain component near the top surface of the steel plate. The neutron diffraction data were obtained at the plane of $z$=-2 mm beneath the surface, whereas the finite element analysis results were for the $z$=-1.5 and -3.0 mm planes, respectively. Note that the neutron diffraction data actually represent averaged values of a 2 mm thick layer. Overall, the finite element results and the neutron diffraction data are consistent in terms of the general strain distribution patterns as well as the magnitude of the strains. According to the calculation, the maximum and minimum longitudinal elastic strains are about $14\times10^{-4}$ and $-8\times10^{-4}$, respectively, whereas the corresponding measured values are $12\times10^{-4}$ and $-6\times10^{-4}$. The transitions from tension strain zone to compression strain zone are also comparable. The region that exhibits the largest differences is located beneath the weld where the FE model overpredicts the measured values. One possible reason is due to the neglect of the dilution effect of weld metal in the FE model, which may significantly alter the mechanical properties of the weld metal and thus the stress equilibrium in the surrounding regions. It should be noted that the mechanical properties of FeAl alloy are generally very sensitive to the chemical composition changes. Another possible cause could be that experimental conditions were not well controlled during the manual welding.

Comparisons between the transverse elastic strain component in the steel plate are illustrated in Figure 4. Only half of the plate was measured with neutron diffraction. Again, the FE model was able to predict the general distribution patterns and magnitudes of the transverse strains as measured by neutron diffraction. A noticeable difference was in the region beneath the weld start where high tensile strains were measured whereas moderate compression strains were calculated. Further study is being conducted to reveal the causes of such discrepancy.

### Residual Stress Distributions

The finite element model predictions of the overall residual stress distributions in both the steel plate and the FeAl weld are shown in Figure 5. The normal stress component $\sigma_{zz}$ is small everywhere in the specimen. As for the longitudinal stress component $\sigma_{yy}$, the FeAl weld metal experiences high and uniform tensile stress. The regions in the steel plate beneath the weld also show tensile stress. High tensile residual stresses in the base steel plate around the weld toes at both weld ends are clearly observed, indicating these regions are preferred failure sites from the stress view point. Particularly, in comparison with the starting end of the weld, greater tensile stress concentration

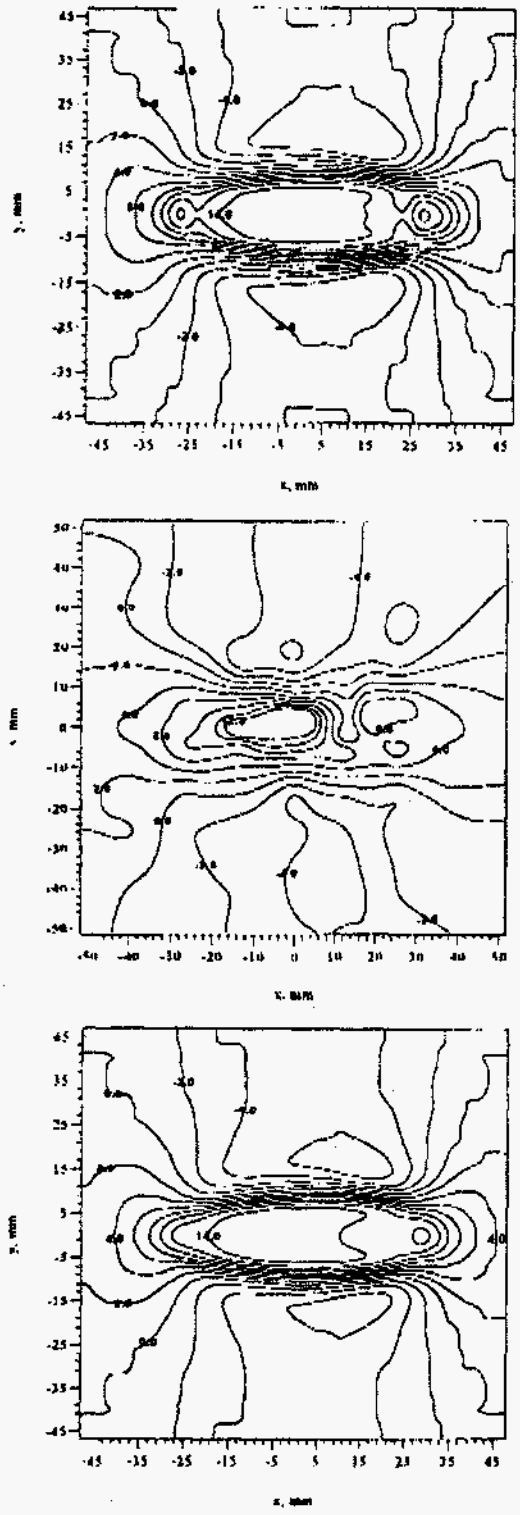

**Figure 3 Comparison of longitudinal elastic strain contours in steel plate (x10,000); Top: FEM results in the plane 1.5 mm from FeAl/steel interface, Middle: Neutron mapping at 2 mm, Bottom: FEM results at 3 mm**

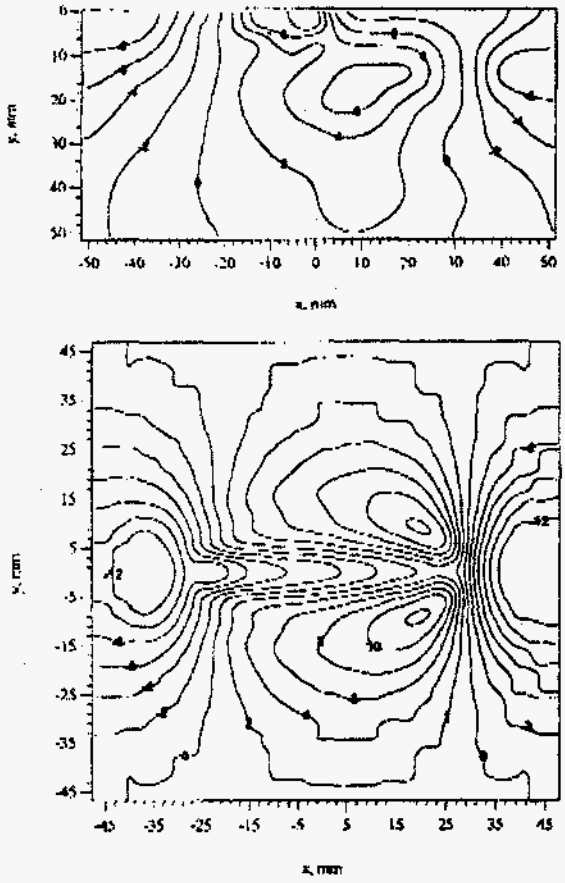

**Figure 4 Comparison of the transverse elastic strains (x10,000); Top: Neutron mapping at 2 mm depth, Bottom: FEM results at 1.5 mm depth.**

appears in the steel plate near the finishing end. This is consistent with the observation that the finishing end of a weld is more susceptible to fatigue crack initiation.

The distribution of the transverse stress $\sigma_{zz}$ is quite different. The magnitude and the sign of the transverse stress depend strongly upon the location in the region beneath the weld. High tensile stresses are concentrated around the finishing end of the weld, whereas the transverse stresses around the starting end of the weld are low, or even in compression. There is also significant in-plane shear stress $\sigma_{xz}$ around both ends of the weld. But it diminishes around the middle section of the weld. Clearly, the strong asymmetric distribution of the transverse and in-plane shear stresses indicates the necessity of using three-dimensional models.

## SUMMARY

In this study, the residual stress field of FeAl cladding on a 2-1/4Cr-1Mo steel was simulated using the finite element model in which the continuous deposition of FeAl during welding was simulated. The computed elastic strain distributions are generally consistent with the neutron diffraction mapping results.

Both the finite element analysis and the neutron diffraction measurement reveal that tensile longitudinal stresses exist in the weld metal and the surrounding areas. The distribution of the transverse stress is highly dependent upon the location. Particularly, there are high tensile longitudinal and transverse residual stresses around the weld toe at the ends of the weld.

The strong spatial dependency of transverse and in-plane shear stress along the weld direction indicates the two-dimensional cross-section models are no longer applicable and three dimensional models have to be used in order to obtain valid residual stress information at the weld end regions where crack initiation is often observed.

## ACKNOWLEDGMENT

This work was supported by the U. S. Department of Energy, Assistant Secretary for Energy Efficiency and Renewable Energy, Office of Industrial Technologies, Advanced Industrial Materials Program and by the Office of Transportation Technology, as part of the High Temperature Materials Laboratory User Programs under contract DE-AC05-96OR22464, managed by Lockheed Martin Energy Research Corp.

## REFERENCES

Argyris, J.H., Szimmat, J. and William, K.J., 1982, "Computational Aspects of Welding Stress Analysis," *Computer Methods in Applied Mechanics and Engineering*, Vol. 33, pp. 635-666.

ASM International, 1990, *Metals Handbook*, Vol. 1, 10th Edition, pp. 617-652.

Dighde, R.M., Meekisho, L.L., Atteridge, D.G. and Wood, W.E., 1993, "Thermal Stress Analysis of the Tekken Weldability Test by the Finite Element Method," *Proceedings, Int. Conf. on Modeling and Control of Joining Processes*, T. Zacharia, ed., American Welding Society, Miami, FL, pp. 558-565.

Feng, Z., Zhu, Y.Y., Zacharia, T., Fields, R.J., Brand, P.C., Prask, H.J. and Blackburn, J.M., 1995, "Modeling and Validation of Residual Stress Distribution in an HSLA-100 Disk," *4th Int. Conf. on Trends in Welding Research*, ASM International, Materials Park, OH, in publication.

Goldak, J., Chakravarti, A. and Bibby, M., 1984, "A New Finite Element Model for Welding Heat Sources," *Metall. Trans.* Vol. 15B, pp. 299-305.

Goldak, J., Oddy, A., McMill, M., Chakravarti, A., Bibby, M. and House, R., 1986, "Progress in Computing Residual Stress and Strain in Welds," *Advances in Welding Science and Technology*, ed. David, S.A., ASM International, Materials Park, OH, pp. 523-527.

Goldak, J., 1989, "Modeling Thermal Stresses and Distortions in Welds," *Recent Trends in Welding Science and Technology*, ed. David, S.A. and Vitek, J.M., ASM International, Materials Park, OH, pp. 71-82.

Hibbitt, H.D. and Marcal, P.V., 1973, " A Numerical, Thermo-Mechanical Model for the Welding and Subsequent Loading of a Fabricated Structure," *Computers & Structures*, Vol. 3, pp. 1145-1174.

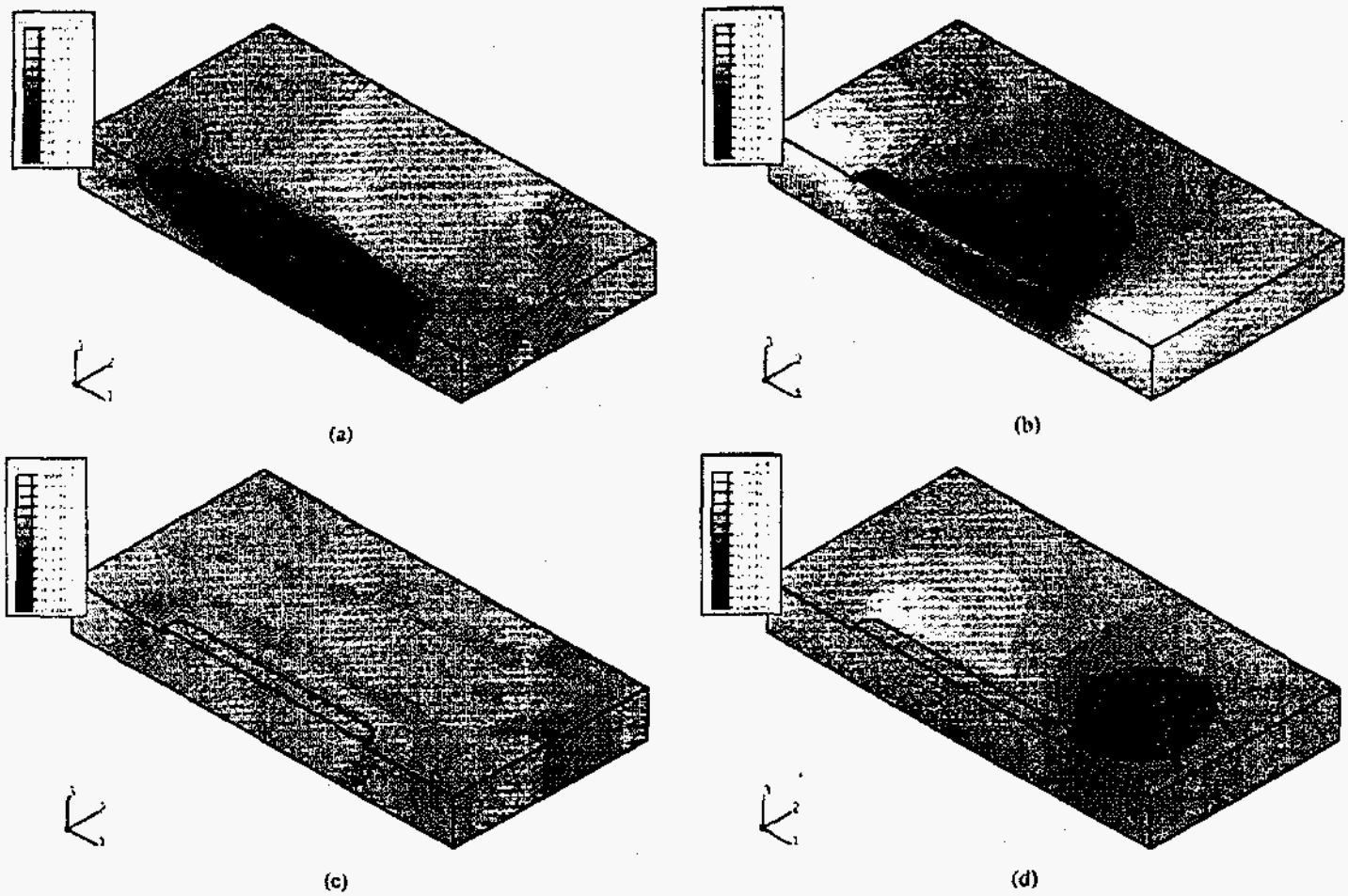


**Figure 5 Residual stress distributions obtained from the finite element analysis in the FeAl weld overlay and steel plate. One half of the plate with a cut through the weld centerline is shown due to symmetry. (a) Longitudinal $\sigma_{11}$ (b) Transverse $\sigma_{22}$ (c) Normal $\sigma_{33}$ (d) In-plane shear $\sigma_{12}$**

Josefson, B.L., 1986, "Stress Distribution during Local Annealing of a Multi-pass Butt-Welded Pipe," *J. of Pressure Vessel Technology*, Vol. 108, pp. 125-130.

Karlsson, R.I. and Josefson, B.L., 1990, "Three-Dimensional Finite Element Analysis of Temperature and Stresses in a Single-Pass Butt-Welded Pipe," *J. of Pressure Vessel Technology*, Vol. 112, pp. 76-84.

Lindgren, L.E. and Karlsson, L., 1982, "Deformations and Stresses in Welding of Shell Structures," *Int. J. Num. Meth. Eng.* Vol. 25, pp. 635-655.

Leung, C.K. and Pick, R.J., 1990, "Finite Element Analysis of Multipass Welds," *Welding Research Council Bulletin 356*, pp. 11-33.

Mahin, K.W., Winters, W., Holden, T.M, Hosbons R.R. and MacEwen, S.R., 1991, "Prediction and Measurement of Residual Elastic Strain Distributions in Gas Tungsten Arc Welds," *Welding J.* Vol. 70, pp. 245s-260s.

Maziasz, P.J., Goodwin, G.M., Liu, C.T. and David, S.A., 1992, "Effects of Minor Alloying Elements on the Welding Behavior of FeAl Alloys for Structural and Weld-Overlay Cladding Applications," *Scripta Metall. Mat.*, Vol. 27, pp. 1835-1840.

Porter, W.D. and Maziasz, P.J., 1993, "Thermal Expansion Data on Several Iron- and Nickel-Aluminide Alloys," *Scripta Metall. Mat.*, Vol. 29, pp. 1043-1048.

Root, J.H., Holden, T.M., Schröder, J., Spooner, S., Hubbard, C.R., Dodson, T.A. and David, S.A., 1993, "Residual Stresses in a Multipass Ferrite Weldment," *Proc. 3rd Int. Conf. on Trends in Welding Research*, ed., David, S.A. and Vitek, J.M., ASM International, Materials Park, OH, pp. 99-103.

Schneibel, J.H., 1994, "Selected Properties of Iron Aluminides," *Processing, Properties, and Applications of Iron Aluminides*, ed., J. H. Schneibel and M. A. Crimp, TMS, Warrendale, PA, pp. 329-42.

Shim, Y., Feng, Z., Lee, S., Kim, D.S., Jaeger, J., Paparitan, J.C. and Tsai, C.L., 1992, "Determination of Residual Stress in Thick-Section Weldments," *Welding J.* Vol. 71, pp. 305s-312s.

Spooner, S., David, S.A., Root, J.H., Holden, T.M., Bourke, M.A.M. and Goldstone, J.A., 1993, "Residual Stress and Strain

Measurements in an Austenitic Steel Plate Containing a Multipass Weld," *Proc. 3rd Int. Conf. on Trends in Welding Research*, ed., David, S.A. and Vitek, J.M., ASM International, Materials Park, OH, pp. 139-143.

Tekriwal, P. and Mazumder, J., 1989 "Thermomechanical Analysis of Residual Strains and Stresses in a GMA Weld," *Recent Trends in Welding Science and Technology*, ed. David, S.A. and Vitek, J.M., ASM International, Materials Park, OH, pp. 91-95

Wang, X.-L., Spooner, S., Hubbard, C.R., Maziasz, P.J., Goodwin, G.M., Feng, Z. and Zacharia, T., 1995, "Residual Stress Distribution in FeAl Weld Overlay on Steel," *Mat. Res. Soc. Symp.*, Vol. 364, pp. 109-114.

## DISCLAIMER